iScience

CellPress

Article

Evolution and Developmental Diversity of Skin Spines in Pufferfishes

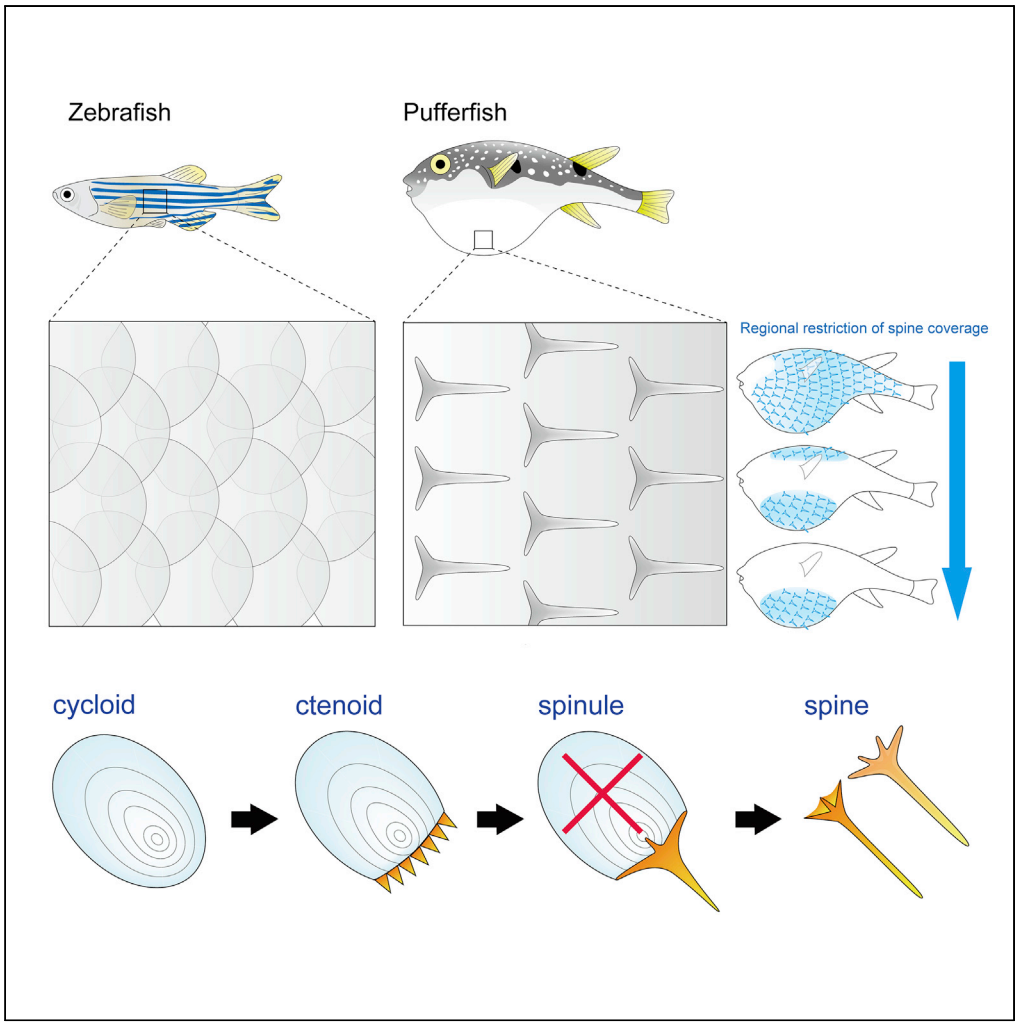

Takanori Shono, Alexandre P. Thiery, Rory L. Cooper, Daisuke Kurokawa, Ralf Britz, Masataka Okabe, Gareth J. Fraser

g.fraser@ufl.edu

HIGHLIGHTS

Tetraodontiformes are highly derived teleosts with extremely modified skin appendages

Pufferfish have skin appendages of single spines and no scale compartment

Pufferfish show variation in spine coverage, from complete to ventral restriction

Conserved signaling regulates formation of scale-less, derived spines in pufferfish

Shono et al., iScience ■■, 1–12
■■, 2019
https://doi.org/10.1016/j.isci.2019.06.003

Please cite this article in press as: Shono et al., Evolution and Developmental Diversity of Skin Spines in Pufferfishes, iScience (2019), https://doi.org/10.1016/j.isci.2019.06.003

iScience

CellPress

Article

Evolution and Developmental Diversity of Skin Spines in Pufferfishes

Takanori Shono,[1,4] Alexandre P. Thiery,[1] Rory L. Cooper,[1] Daisuke Kurokawa,[2] Ralf Britz,[3] Masataka Okabe,[4] and Gareth J. Fraser[1,5,6,*]

SUMMARY

Teleost fishes develop remarkable varieties of skin ornaments. The developmental basis of these structures is poorly understood. The order Tetraodontiformes includes diverse fishes such as the ocean sunfishes, triggerfishes, and pufferfishes, which exhibit a vast assortment of scale derivatives. Pufferfishes possess some of the most extreme scale derivatives, dermal spines, erected during their characteristic puffing behavior. We demonstrate that pufferfish scale-less spines develop through conserved gene interactions that underlie general vertebrate skin appendage formation, including feathers and hair. Spine development retains conservation of the EDA (ectodysplasin) signaling pathway, important for the development of diverse vertebrate skin appendages, including these modified scale-less spines of pufferfish. Further modification of genetic signaling from both CRISPR-Cas9 and small molecule inhibition leads to loss or reduction of spine coverage, providing a mechanism for skin appendage diversification observed throughout the pufferfishes. Pufferfish spines have evolved broad variations in body coverage, enabling adaptation to diverse ecological niches.

INTRODUCTION

Vertebrates possess a huge diversity of skin appendages, including teleost fish scales, reptilian scales, avian feathers, and mammalian hair (Pispa and Thesleff, 2003). Although these units are not structurally homologous, the genetic control of their early development appears to be highly conserved between diverse vertebrate clades (Musser et al., 2015; Di-Poï and Milinkovitch, 2016; Cooper et al., 2017). Vertebrate skin appendages broadly originate from a conserved anatomical placode (Di-Poï and Milinkovitch, 2016), before divergence in morphogenesis gives rise to a plethora of disparate adult structures. This process is underpinned by inductive epithelial-mesenchymal interactions, mediated by a conserved set of signaling molecules. These include the hedgehog (Hh), Wnt, bone morphogenetic protein (BMP), fibroblast growth factor (FGF), Notch, and ectodysplasin A (EDA) pathways (Biggs and Mikkola, 2014).

Although the diversity of skin ornaments in teleost fishes is vast, our knowledge of their development is limited. Skin appendages in tetrapod lineages arise from epithelial cells of ectodermal origin (Di-Poï and Milinkovitch, 2016), whereas teleost scales primarily arise from underlying mesodermal layers of the dermis (Shimada et al., 2013; Mongera and Nüsslein-Volhard, 2013). Previous research has demonstrated that the Hh, Fgf, Bmp, Wnt/β-catenin and Eda pathways are involved in teleost scale development (Kondo et al., 2001; Sire and Akimenko, 2004; Harris et al., 2008; Iwasaki et al., 2018; Albertson et al., 2018; Aman et al., 2018). Signaling of *eda* and its receptor, *edar*, also control the morphology and patterning of the body plate armor of marine and freshwater stickleback (Colosimo et al., 2005; O' Brown et al., 2014). It is likely that even the most extremely modified teleost skin ornaments share elements of these core signaling pathways, known to underpin skin appendage development throughout diverse vertebrate groups.

Tetraodontiformes include a range of remarkable teleost fishes, such as ocean sunfishes (Molidae), triggerfishes (Balistidae), and pufferfishes (Tetraodontidae). The ~350 species of this highly derived order exhibit extreme morphological diversification, both in terms of their craniofacial and dermal skeletons (Santini and Tyler, 2003; Fraser et al., 2012; Thiery et al., 2017). Members of each of the tetraodontiform clades possess striking mineralized integumentary appendages, ranging from spinoid scales to individual spines and thick, plate-like armor (Figure 1). Dermal scale development in the Tetraodontiformes is thought to be associated with evolution and modification of the typical squamous scale types (e.g., cycloid, spinoid, or ctenoid) found in most teleost fishes (Roberts, 1993). However, evolutionary developmental approaches have not been used to test this hypothesis.

[1]Department of Animal and Plant Sciences, Bateson Centre, University of Sheffield, Sheffield S10 2TN, UK

[2]Misaki Marine Biological Station, School of Science, University of Tokyo, Miura, Kanagawa 238-0225, Japan

[3]Department of Life Sciences, Natural History Museum, London SW7 5BD, UK

[4]Department of Anatomy, The Jikei University School of Medicine, Minato, Tokyo 105-8461, Japan

[5]Department of Biology, University of Florida, Gainesville 32611, USA

[6]Lead Contact

*Correspondence: g.fraser@ufl.edu

https://doi.org/10.1016/j.isci.2019.06.003

Please cite this article in press as: Shono et al., Evolution and Developmental Diversity of Skin Spines in Pufferfishes, iScience (2019), https://doi.org/10.1016/j.isci.2019.06.003

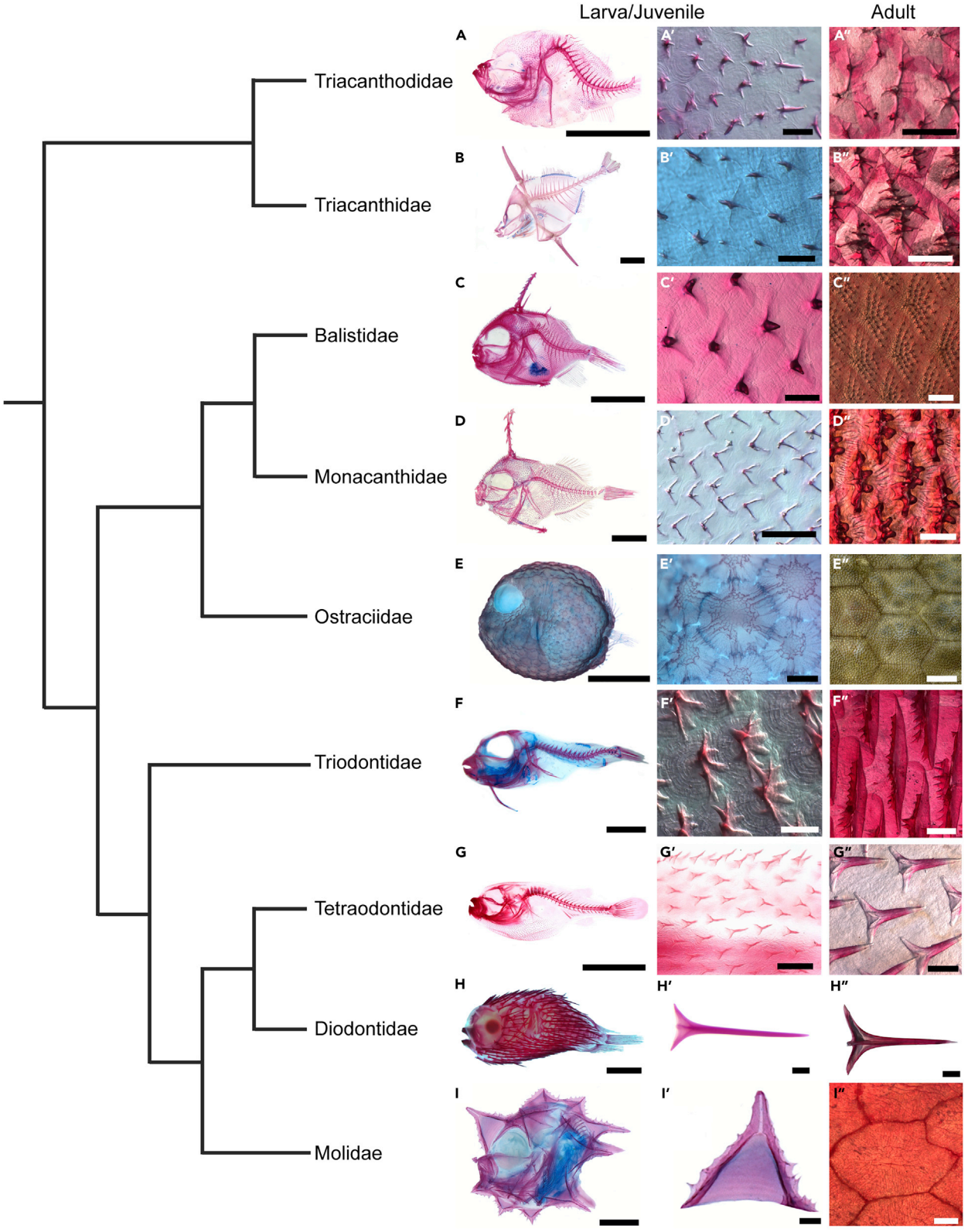

Please cite this article in press as: Shono et al., Evolution and Developmental Diversity of Skin Spines in Pufferfishes, iScience (2019), https://doi.org/10.1016/j.isci.2019.06.003

Figure 1. Skin Appendage Diversity in the Order Tetraodontiformes

Cleared and stained spinoid scales and spines of larvae/juveniles and adults in representative species of tetraodontiform families.
(A) Triacanthodidae, *Hollardia* sp., Standard Length (SL); 5mm (A and A′) and *Paratriacanthodes herrei*, SL; 42.5 mm (A″).
(B) Triacanthidae, *Tripodichthys oxycephalus*, SL; 4, 26 mm (B and B′) and *Pseudotriacanthus strigilifer* SL; 88 mm (B″).
(C) Balistidae, *Balistes vetula*, SL; 10 mm (C and C′) and *B. capriscus*, SL; 128 mm (C″).
(D and E) (D) Monacanthidae, *Stephanolepis* sp., SL; 5 mm (D and D′) and *S. hispidus* SL; 94.5 mm. (E) Ostraciidae, *Ostracion* sp., SL; 6.2 mm (E and E′) and *Ostracion trigonus*, SL; 330 mm (E″).
(F) Triodontidae, *Triodon macropterus*, SL; 20 mm (F and F′) and *T. macropterus* SL; 315 mm (F″).
(G) Tetraodontidae, *Takifugu niphobles*, 10 mm (G and G′) and *T. niphobles*, SL; 102.3 mm (G″).
(H) Diodontidae, *Diodon holocanthus*, SL; 12.5 mm (H and H′) and *D. holocanthus* SL; 101 mm (H″).
(I) Molidae, *Ranzania laevis*, SL; 1.7 mm (I and I′) and *R. laevis*, SL; 620 mm (I″). Phylogenetic relationships of tetraodontiform families follow a published dataset (Santini and Tyler, 2003), which combined data from both extinct and extant members of the Tetraodontiformes to build the phylogeny.
Scale bars, 2 mm (A, C, D, E, G, and H), 500 μm (A′, A″, B″, G″, and I) 5 mm (B and F), 100 μm (B′, C′, D′, F′, G′, H′, and I′), 1 mm (C″, E″, F″, H″, and I″), and 200 μm (D″ and E′).

Pufferfishes (Tetraodontidae) possess a diverse range of body spines, which provide a powerful defense mechanism. The *Takifugu* pufferfish lineage is well known from recent genome sequencing efforts that demonstrated that pufferfishes represent vertebrates with the smallest known, most compact genome. Furthermore, this lineage has undergone a relatively recent explosive radiation (Venkatesh et al., 2000; Jaillon et al., 2004). During this radiation, pufferfish spines diversified in their size and shape, as well as their patterning across the body, which ranges from a complete lack of spines to a dense coverage (Figure 2).

Here, we present (1) information on the diversity and modification of skin ornaments in this particularly morphologically varied order of teleost fishes, the Tetraodontiformes; (2) describe the development of the dermal spines in pufferfish (*Takifugu niphobles*) as a model for skin appendage novelty and diversification; (3) report on the results of developmental and genetic manipulation of the spines that cover the ventral surface of *Takifugu*; and finally (4) suggest an evolutionary mechanism for how morphological diversity of skin ornament in this group may have arisen.

RESULTS

Tetraodontiform Skin Appendages Exhibit Highly Varied Morphologies

There are 10 tetraodontiform families with a diverse array of dermal ornamentations, which vary both in terms of their structure and spatial distribution (Santini and Tyler, 2003; Matsuura, 2014). To examine this morphological diversity, we cleared and stained both juvenile and adult specimens representing extant tetraodontiform families (Figure 1). In the families Triodontidae, Tetraodontidae, and Diodontidae, the morphology and localization of ornamentation are similar between both juvenile and adult specimens (Figure 1). The juveniles of both basal spikefishes (family Triacanthodidae) and the more derived three-toothed pufferfish (family Triodontidae) exhibit mineralized units in the skin that consist of a scale-like plate with one (in triacanthodids) or several (in triodontids) individual spines at the posterior margin. The anterior scale-like plate strongly resembles a typical cycloid scale with concentric ridges or circuli (Figures 1A and 1F). The "cycloid" base in these two groups is still present, although less obvious, in the spinoid scales observed in the adults.

Juveniles of the tripod fishes (family Triacanthidae), the triggerfishes (family Balistidae), and the filefishes (family Monacanthidae) also exhibit a single-spined unit on a "cycloid" base, which appears to lack circuli. In contrast, adults of these three families possess a more complex structure, with spines or spinules sometimes covering the entire visible scale surface (Figures 1C and 1D). Boxfishes (family Ostraciidae) do not possess any spines but instead have a covering of separate hexagonal bony plates on the body surface of juveniles, which grow together to form a thick armor in adults (Figure 1E).

Pufferfishes (family Tetraodontidae) and porcupine fishes (family Diodontidae) possess individual spines that vary in their patterning between different species. Porcupine fishes have particularly long spines covering their entire body, whereas the smaller spines of pufferfishes range from forming a complete coverage of the entire body (seen in *Carinotetraodon*; Britz et al., 2012) to being restricted to specific ventral and/or dorsal regions (Figure 2). In *Takifugu niphobles*, these spines are restricted to the dorsal head and ventral abdominal regions. Individual spines of pufferfishes are composed of a basal multi-pronged root embedded into the dermis and a distally pointed single spine tip (Figures 1G and 1H). Juvenile ocean sunfish (family Molidae) are covered with a network of jagged-edged pyramidal spines covering the skin, whereas adults have no spines, but instead their entire body is covered with polygonal scale-like

Please cite this article in press as: Shono et al., Evolution and Developmental Diversity of Skin Spines in Pufferfishes, iScience (2019), https://doi.org/10.1016/j.isci.2019.06.003

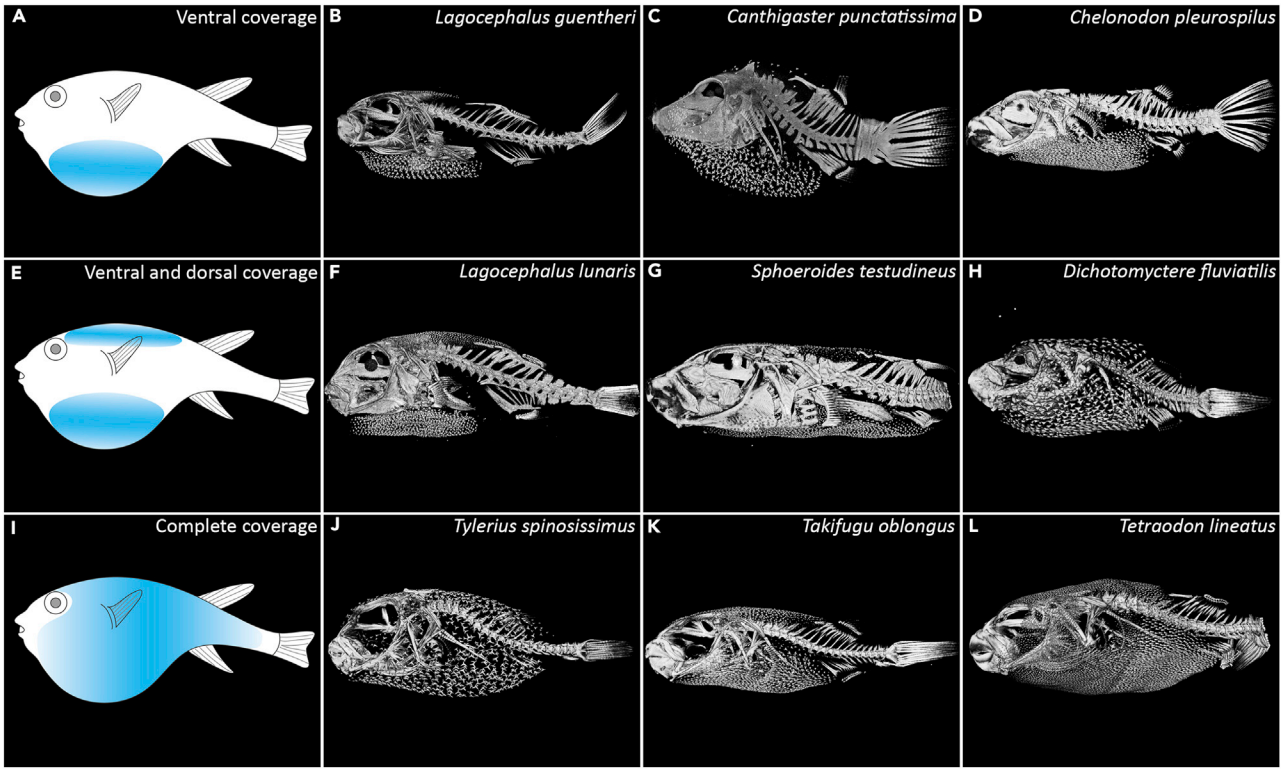

Figure 2. Spine Diversity of the Tetraodontidae

Computed tomography (CT) renders of Tetraodontidae species, *Lagocephalus guentheri* (B), *Canthigaster punctatissima* (C), *Chelonodon pleurospilus* (D), *Lagocephalus lunaris* (F), *Sphoeroides testudineus* (G), *Dichotomyctere fluviatilis* (H), *Tylerius spinosissimus* (J), *Takifugu oblongus* (K) and *Tetraodon lineatus* (L). The coverage of spines in the species are ranging from (A) ventrally restricted in B–D, (E) dorsal and ventral in F and G, and (I) complete in H, J, K, and L. All CT data acquired from MorphoSource digital 3D media repository.

plates (Figure 1I) (Katayama and Matsuura, 2016). Overall, Tetraodontiformes show a huge diversity in dermal ornamentations (see Table S1 for a summary of observations). For this reason, they are particularly well suited for the study of the evolutionary and developmental basis of the diversification of body ornamentation.

Pufferfish Spines Develop from Mesenchymal Condensations

Morphological descriptions of spinoid scales, plates, and spines have previously been reported, predominantly for adult Tetraodontiformes (Roberts, 1993; Santini and Tyler, 2003; Gauldie, 1992). However, the developmental basis of their diversity remains poorly understood. Therefore, we investigated the development of spines of the Japanese Grass Pufferfish (*Takifugu niphobles*; Tetradontidae).

Scanning electron microscopy revealed a localized region of skin protrusions between the ventral pectoral girdle and the abdominal region at 12 days post fertilization (dpf) (Figure 3A). The ectodermal units that project from the body surface at this stage mark the spines' initial site of development (Figure 3B). Sagittal sections of embryos at 13 dpf demonstrated that developing spine regions are composed of two tissue layers, epithelium and mesenchyme, and associated pigment cells, including melanocytes. The spine primordia are derived from mesenchyme (dermis) and stain strongly with hematoxylin (and Alcian Blue; Figure 3C). In juvenile stages (at 46 dpf), developing spines extend from a fibrous layer of the dermis (Figure 3D). In adult stages, Alizarin red staining shows functional mineralized spines protruding through the outer layers of the skin (Figure 3E). Overall, these results demonstrate that spine development in *Takifugu* initiates from the mesenchyme (dermal mesoderm) during early ontogeny. This bears similarity to the scale development of medaka and zebrafish, although in zebrafish this process begins later in development, at approximately 1 month post fertilization (Kondo et al., 2001; Le Guellec et al., 2004; Sire and Akimenko, 2004; Shimada et al., 2013; Mongera and Nüsslein-Volhard, 2013).

Please cite this article in press as: Shono et al., Evolution and Developmental Diversity of Skin Spines in Pufferfishes, iScience (2019), https://doi.org/10.1016/j.isci.2019.06.003

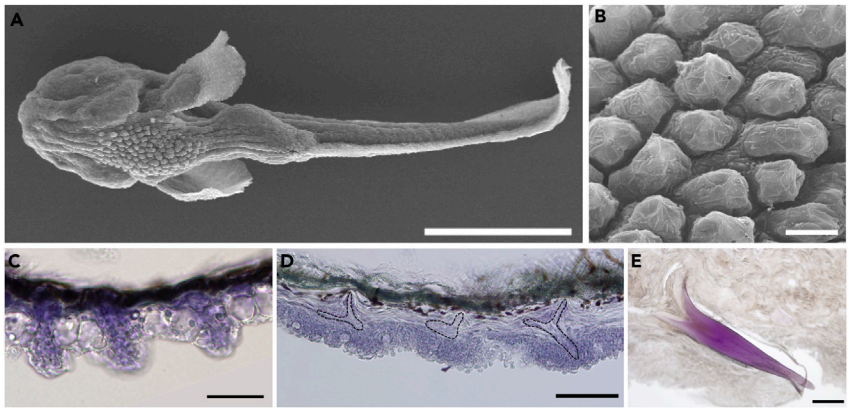

Figure 3. Location and Histological Structure of Spines of *Takifugu*

(A) Scanning electron microscopy of ventral bossy surface of *Takifugu niphobles*, 12 dpf.

(B) Close-up of spine regions.

(C) Sagittal sections of spine regions in 13 dpf of an embryo stained with Hematoxylin and Alcian Blue staining.

(D) Sagittal section of spines in 46 dpf embryo stained with Hematoxylin. Black dotted lines indicate spines.

(E) Sagittal section of spines in an adult stained with Alizarin Red. Scale bars, 500 μm (A), 20 μm (B), 50 μm (C and D), and 200 μm (E).

Conserved Molecular Pathways Underlie in Spine Development in the Pufferfish

Having observed this similarity between *Takifugu* spine development and scale development of other teleost fishes (Shimada et al., 2013; Mongera and Nüsslein-Volhard, 2013), we sought to investigate the genetic pathways that underlie spine formation in this pufferfish. Therefore, we selected a suite of important signaling pathways (including Wnt/β-catenin, Hh, FGF, and BMP) that underlie ectodermal appendage development throughout diverse vertebrates and chartered their expression during *Takifugu* spine development (Pispa and Thesleff, 2003; Di-Poï and Milinkovitch, 2016).

β-Catenin is a signal transducer of canonical Wnt signaling, a pathway known to play important roles in cell proliferation and differentiation during organogenesis of various structures (Grigoryan et al., 2008). We observed expression of *β-catenin* within both the epithelium and mesenchyme of the spine primordium, with stronger expression at the boundary region between primordia and the overlying epithelium (Figure 4A). We also observed expression of the transcription factor *lef1* (Lymphoid enhancer binding factor-1), which is associated with the canonical Wnt pathway by interaction with *β-catenin* (Hovanes et al., 2001), in the distal region of the primordium epithelium (Figure 4B). Expression of *lef1* is consistent throughout the early regional specification that demarcates spine competent ectoderm, with its expression upregulated at the border of the ventrally restricted spine-forming region (Figure 4B). The Wnt pathway ligand, *wnt7a*, of the frizzled family of transmembrane receptors (Vogel et al., 1995), is expressed throughout both the mesenchymal and epithelial compartment, although its expression is stronger at the distal tip (at the apex of the spine) of the epithelium where the spine forms (Figure 4C).

shh, a ligand of the Hh pathway, has a critical role in cell division, specification, and patterning of organs (Varjosalo and Taipale, 2008). We observed *shh* expression in the epithelium adjacent to spine primordia (Figure 4D). This expression pattern bears similarity to zebrafish scale development, where *shh* is expressed in the epithelium adjacent to the scale anlagen (Sire and Akimenko, 2004).

Sostdc1 (Sclerostin domain-containing 1, also known as *Wise*, *ectodin*, and *USAG-1*) encodes an N-glycosylated secreted protein, associated with the BMP pathway as an antagonist, and mediates regulation of the network for both the Hh and Wnt pathways (Yanagita, 2004; Ahn et al., 2010). We observed expression of *sostdc1* in the ventral spine region and restricted to the distal end of the spine primordium (Figure 4E).

FGF ligands play a key role in the processes of proliferation and differentiation in various organs, interacting with Hh, Wnt, and BMP signaling pathways (Neubüser et al., 1997). *fgf3* is expressed in the epithelial cells adjacent to the distal tip of spine primordia in *Takifugu* (Figure 4F). In contrast, *fgf10a* is expressed extensively in the epithelium, with stronger expression observed in the epithelium adjacent to the distal

Please cite this article in press as: Shono et al., Evolution and Developmental Diversity of Skin Spines in Pufferfishes, iScience (2019), https://doi.org/10.1016/j.isci.2019.06.003

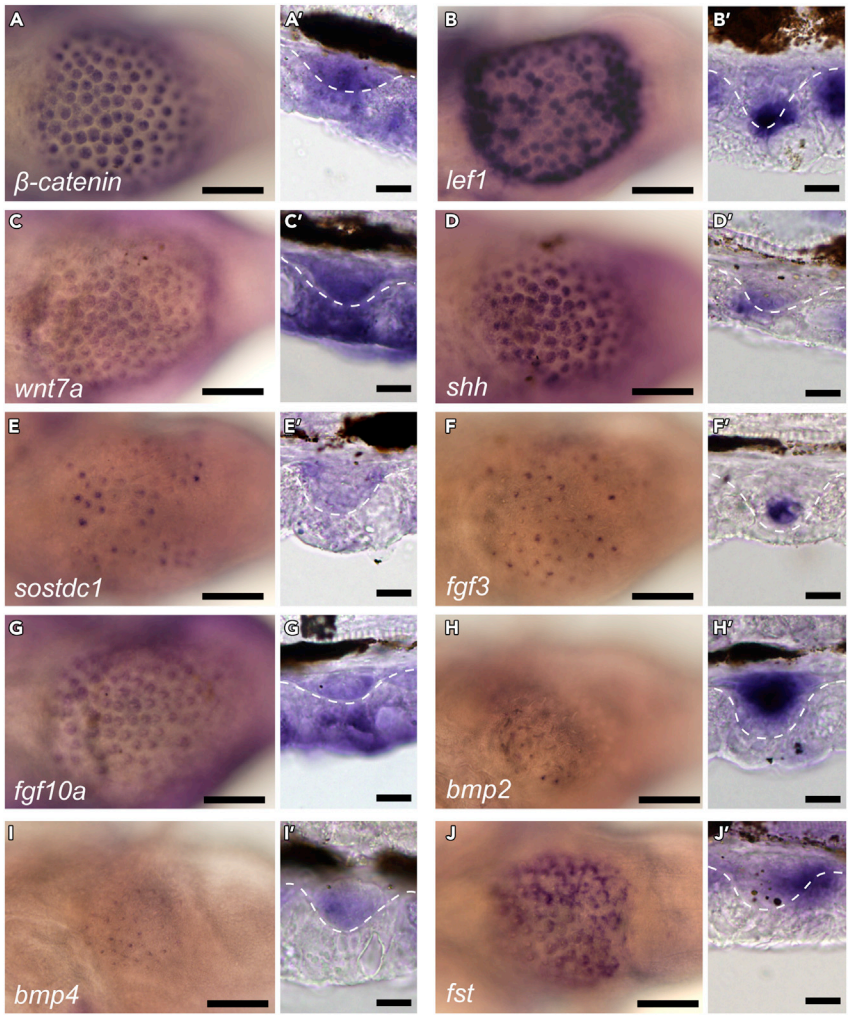

Figure 4. Gene Expression in Embryonic Spine Primordia of *Takifugu* at 12 dpf

Gene expression for *β-catenin* (A), *lef1* (B), *wnt7a* (C), *shh* (D), *sostdc1* (E), *fgf3* (F), *fgf10a* (G), *bmp2* (H), *bmp4* (I), and *fst* (J). Right each panel (A′–J′) shows images of spine primordia in sagittal section. White dotted line indicates a boundary line between spine primordia and epithelium layer. Scale bars, 100 μm (A–J) and 10 μm (A′–J′).

tip of spines (Figure 4G). The BMP pathway is involved in a variety of cellular interactions during various organogenic processes, including antagonism of the FGF signaling pathway (Neubüser et al., 1997; Shi and Massagué, 2003). The Bmp ligands *bmp2* and *bmp4* are both expressed in the spine primordium and, importantly, in a pre-patterned ventral region before spine placode formation, demarcating the restricted field where spines will form (Figures 4H and 4I). This suggests Bmp signaling may be important in initiating a spine competent dermis in *Takifugu*. Follistatin (FST) is an activin-binding protein known to antagonize BMP signaling (Bauer et al., 1998; Thompson et al., 2005). We observed *fst* in the mesenchyme surrounding each spine primordia (Figure 4J). Overall, these results highlight that conserved markers of vertebrate ectodermal appendage formation are expressed and active during the initiation, development, and organization of the highly derived spine ornament of pufferfishes (Figure S1).

Gene Knockdown Assays Suggest the BMP Pathway Controls Patterning of Takifugu Spines

BMP signaling is known to regulate the number, pattern, and sizes of diverse vertebrate skin appendages (Jung et al., 1998; Jiang et al., 1999; Mou et al., 2006; Plikus et al., 2008). Therefore, we investigated the role of the Bmp pathway in regulating dermal spine patterning in *Takifugu*. At 10 dpf, before spine initiation, *bmp2* and *bmp4* are expressed in the ventral mesenchyme, defining the restricted region in which spines can form (Figures 5A and 5B). To identify the functional role of the Bmp pathway in spine development, we

Please cite this article in press as: Shono et al., Evolution and Developmental Diversity of Skin Spines in Pufferfishes, iScience (2019), https://doi.org/10.1016/j.isci.2019.06.003

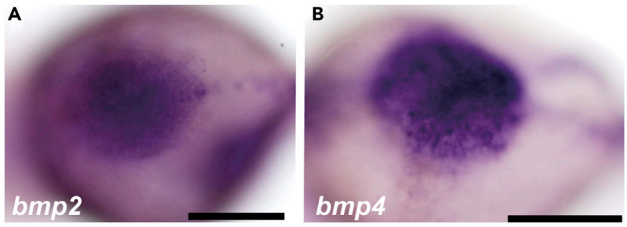

Figure 5. BMP Signaling Genes Demarcate Spine Competent Region in *Takifugu* during Early Development
Ventral view of 10 dpf embryos. During initiation of spine development, *bmp2* (A) and *bmp4* (B) are expressed in a specific region of ventral (abdominal) mesenchyme. Scale bar, 200 μm.

undertook Bmp gene knockdown assays through injection of an antisense morpholino (MO), in fertilized *Takifugu* eggs at the one-cell stage.

Although injections with *bmp2* or *bmp4*-MO resulted in mortality at the hatchling stage (6 dpf), morphants injected with *fst*-MO, an antagonist of BMP, continued to develop. These *fst*-MO morphants exhibited perturbed jaw development at 12 dpf (Figures S2A and S2B). Similar to experiments undertaken on zebrafish (Dal-Pra et al., 2006), Alcian blue staining revealed abnormal arrangement of Meckel's cartilages in *fst*-MO *Takifugu*, with the formation of only four branchial arches, rather than the normal set of five (Figures S2C and S2D). Treatment with *fst*-MO also perturbed normal development of *Takifugu* spines. Spines are normally present in the ventral region of *Takifugu*. However, in morphant embryos injected with *fst*-MO, hyperplasia of spines was observed (Figures S2E and S2G). Furthermore, the distal tip of spines developed earlier in *fst*-MO morphants than in control embryos (Figures S2F and S2H). We also documented a reduction in spine number in the ventral region (per 2 mm^2) in *fst*-MO morphants, compared with wild-types (Figure S2I). Despite an expansion of the ventral spine-competent region *Takifugu* morphants, the overall number of spines was reduced. Overall, these results suggest that Bmp pathway–associated *fst* controls pufferfish spine patterning, influencing both the size of the spine-competent field and the patterning of spines within this region.

Small-Molecule Gene Inhibition Experiments Reveal Functional Conservation of Signaling Pathways

Pufferfish spine development involves members of the Hh, Bmp, Wnt, and Fgf signaling pathways (Figures 4 and S3). To understand the function of these pathways, and also the potential role of Notch, a transmembrane receptor that mediates cell communication and fate (Lai, 2004), we undertook small-molecule gene inhibition experiments to inhibit specific gene signaling. After hatching, embryos were exposed to small molecules for 72 h, covering the initiation, patterning, and primordium formation stages of spine development. Control embryos were treated with 1% DMSO. Following treatment, embryos developed under standard conditions for a further 14 days, before Alcian blue staining was used to observe phenotypic shifts (Figure 6A).

Treatment with the Hh antagonist Cyclopamine (Incardona et al., 1998) (50 μM) severely repressed spine formation in the ventral region (Figure 6B), indicating Hh signaling is essential for normal development. Additionally, treatment with the BMP inhibitor LDN193189 (Cuny et al., 2008) (5 μM) and the FGF receptor inhibitor SU5402 (Mohammadi et al., 1997) (50 μM) resulted in a small reduction in ventral spine number (Figure 6L). Treatment with the Wnt inhibitor, IWR-1-endo, mostly resulted in lethality of embryos (1 μM); however, a single individual survived the treatment and displayed a severe reduction in the number of spines (Table S2). Furthermore, treatment with the γ-secretase complex and Notch pathway inhibitor, DAPT (Geling et al., 2002) (25 μM), resulted in abnormal spine morphogenesis and a 40% reduction in spine number in the ventral region of *Takifugu* (Figures 6C and 6L). This suggests the Notch pathway is required for normal spine development and led us to examine the expression of Notch pathway members. We observed the Notch ligand *notch3* in the ventral spine-forming region of *Takifugu* at 10 dpf, although expression was not specifically restricted to spine primordia (Figure 6D). This same region was also found to strongly express *shh* (Figure 6E).

In situ hybridization following small-molecule treatments revealed that cyclopamine and DAPT affected the activity of other important signaling pathways, including the Bmp and Wnt pathways, 72 h post treatment (Figures 6F–6K). Cyclopamine-treated embryos exhibited reduced expression patterns of *bmp2* and *lef1*

Please cite this article in press as: Shono et al., Evolution and Developmental Diversity of Skin Spines in Pufferfishes, iScience (2019), https://doi.org/10.1016/j.isci.2019.06.003

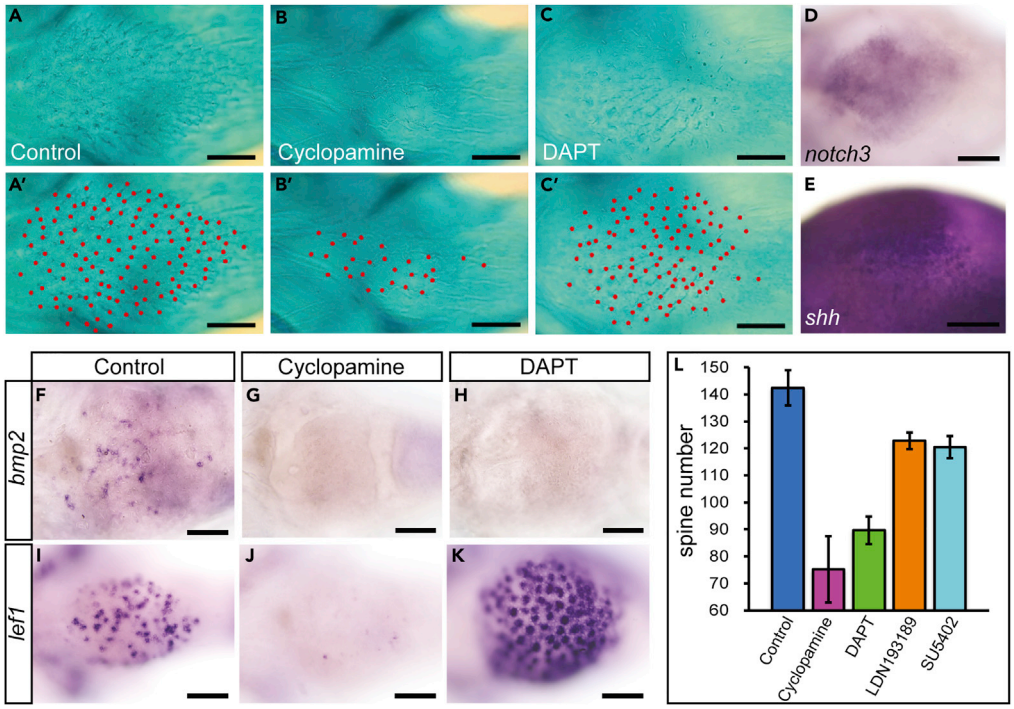

Figure 6. Manipulation of Hh, Notch, BMP, and FGF Pathways during Spine Development

(A–C) Alcian Blue–stained ventral spine of *T. niphobles* embryos treated with small molecules for 72 h and subsequent recovery process until 14 dpf. The treatment is 1% DMSO as a control (A), 50 μM Cyclopamine (B), and 25 μM DAPT (C), respectively. (A′-C′) Ventral spines in each sample marked with dotted red line.

(D and E) Gene expression of *notch3* (D) and *shh* (E) in the ventral region where spines will form by whole-mount RNA *in situ* hybridization of embryos at 10 dpf.

(F–K) Comparison of gene expression in the spines for chemically treated embryos between 1% DMSO control (F and G), 50 μM Cyclopamine (H and I), and 25 μM DAPT (J and K) by whole-mount RNA *in situ* hybridization of embryos past from 72 h treatment. Gene expression for *bmp2* (F, H, and J) and *lef1* (G, I, and K).

(L) Quantitative comparison for the spine total number of 14-dpf embryos between treatment with 1% DMSO control (n = 5), 50 μM Cyclopamine (n = 6), 25 μM DAPT (n = 9), 5 μM LDN193189 (n = 9), and 50 μM SU5402 (n = 10). Data are represented as mean ± SEM. Scale bar, 100 μm.

compared with control embryos (Figures 6F–6J). Treatment with DAPT reduced *bmp2* expression, whereas *lef1* was significantly upregulated in spine primordia, compared with control embryos (Figures 6H–6K).

Overall, these results suggest that conserved signaling pathways associated with the development of other diverse vertebrate ectodermal appendages are also involved in the development of pufferfish spines. The Hh pathway plays a prominent role in the initiation and patterning of spines in *Takifugu* and is important for the regulation of Bmp and Wnt signaling.

edar Is Required for Development and Patterning of Pufferfish Spines

edar is a cell surface receptor for *eda* and plays an important role during the development of diverse vertebrate skin appendages (Kondo et al., 2001; Colosimo et al., 2005; Fessing et al., 2006; Harris et al., 2008). This gene is well characterized in relation to the evolution of stickleback armor patterning (Colosimo et al., 2005; O'Brown et al., 2015). To determine whether *edar* is involved in the development of the related, yet distinct, dermal armor of spines in pufferfishes, we examined *edar* gene expression from embryonic to juvenile stages of *Takifugu*. In the embryonic stage at 12 dpf, *edar* was expressed in the ventral region of the protruding epithelium overlying the spine primordium (Figures S4A–S4C). At the later juvenile stages, expression of *edar* was present in the epidermis, especially in cells adjacent to each distal spine tip (Figure S4D).

To understand the function of *edar* in the development of spines, we next performed gene knockout mutagenesis by CRISPR-Cas9 targeted *edar*. Two guide RNAs (*edar#1* and *edar#2*) were designed targeting

Please cite this article in press as: Shono et al., Evolution and Developmental Diversity of Skin Spines in Pufferfishes, iScience (2019), https://doi.org/10.1016/j.isci.2019.06.003

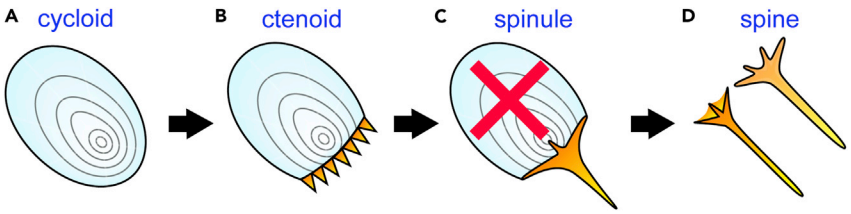

Figure 7. Schematic Representation of Hypothesized Evolution of Tetraodontid and Diodontid Skin Spines from Scales

(A) Basic cycloid scale, of squamous type without ornamentations observed in teleost species.

(B and C) (B) Ctenoid scale with tooth-like spines projecting on the posterior side separate from the main cycloid compartment (Roberts, 1993) (C) Plesiomorphic condition of tetraodontiform spinoid scale, composed of cycloid scale and single projecting spine posteriorly as in larval stages of extant Triacanthodidae, Triacanthidae, Balistidae, Monacanthidae (see Figure 1). During evolution of ancient lineage of Tetraodontidae and Diodontidae (or Molidae; Gymnodontes), cycloid compartment has been lost, but single spines are retained.

(D) Because the EDA signaling pathway has been implicated in the normal formation of the cycloid scale compartment in teleost fishes, it seems plausible that modification of gene pathways such as EDA may have contributed to the developmental changes by which derivative skin appendages can form without the typical teleost "cycloid" scale compartment.

exons of *edar* (Figure S4E). The designed RNAs were co-injected with CAS9 nuclease protein into fertilized eggs. The sequence analyses of DNA fragment harboring target site from injected embryos demonstrated the insertion/deletion (Figures S4F and S4G). We compared expression patterns of *shh* between wild-type and *edar* mutated G0 embryos at 12 dpf. In wild-type embryos, we saw expression of *shh* specific to the spine-forming region, whereas expression patterns for *edar* mutated embryos (*edar#1* and *edar#2*) were irregular (Figure S4H). We also documented reduction in the number of *shh*-positive spines in *edar* mutated embryos, when compared with the number of spines in wild-type (Figure S4I). These results suggest that *edar* has an important role in the proper arrangement and development of the spine competent territory in *Takifugu*.

DISCUSSION

Overall, our results demonstrate that the unique skin ornamentation of the pufferfishes (Tetraodontidae) has likely evolved through changes to the initiatory process of skin appendage patterning. This includes early regional restriction of signaling molecules demarcating competent fields of spine formation. It differs from the typical signaling that instigates an initiatory row from which other appendages propagate, such as zebrafish scales, shark dermal denticles, and avian feather tracts (Sire and Akimenko, 2004; Pan et al., 2004; Cooper et al., 2018). Instead, spine primordia form simultaneously within the territories established by the Hh, Wnt, and Bmp signaling molecules (Figure 4). Similar to feather patterning, where genes associated with these pathways are up-regulated in regions destined to become feather tracts (Jung et al., 1998; Jiang et al., 1999; Pan et al., 2004), we see their expression restricted to the spine-forming region of the pufferfish, albeit in a larger non-sequential domain. Alterations to these expression patterns may have facilitated the modification of this region, enabling diverse species-specific spine patterning to arise (Figure 2). Spine patterning in pufferfishes ranges from a complete coverage of spines in groups such as *Carinotetraodon* to the more restricted coverage of spines in *Takifugu niphobles*. Pufferfishes provide interesting developmental models for studying the regional restriction and elaboration of vertebrate skin appendages.

Morphological variation of tetraodontiform dermal ornamentation is substantial (Figures 1 and 2). Triacanthodidae, the most basal family in the Tetraodontiform phylogeny, possess numerous spines with complex adult morphologies. However, juvenile stages exhibit a single spine that projects from the cycloid compartment of the scale (Figures 1A–1C). Therefore, the common ancestor of the group may have had one (or several) spine(s) attached to a scale with a cycloid base. This hypothesized primitive condition for tetraodontiforms is similar to spinoid scales observed in other teleost groups, where spines project out from the main body of the scale posteriorly as continuations of the cycloid base (Roberts, 1993). Based on our findings and conclusions, we propose a new hypothesis for the morphological evolution of the dermal skeleton in Tetraodontiformes (Figure 7). Members of different families exhibit loss of either the cycloid base (i.e., Tetraodontidae and Diodontidae) or spines (i.e., Molidae and Ostraciidae) from the scale. In molids and ostraciids, we would hypothesize that the cycloid base has been modified into a

thick armor of polygonal plates, which may provide increased protection from predators. When looking at the diversification of spines, the Triacanthodidae, Balistidae, Monacanthidae, and Triodontidae show a "cycloid" base adorned with a varying number of spines, whereas we would suggest that the cycloid compartment has been lost entirely in the Tetraodontidae and Diodontidae. We therefore conclude that spines in the Tetraodontidae and Diodontidae are highly derived dermal elements that are homologous to the standard scales of other teleost fishes (Figure 7) and not neoformations.

The transition to spines in pufferfish and the associated loss of the cycloid compartment in the Tetraodontidae and Diodontidae could have occurred by the modification of the conserved genetic network that operates during cycloid scale development (Colosimo et al., 2005; Harris et al., 2008; O'Brown et al., 2015; Aman et al., 2018; Iwasaki et al., 2018). Specifically, the Eda (ectodysplasin) pathway may have played a crucial role during the diversification of tetraodontiform scales. This pathway is important in refining the size, spacing, and shape of various vertebrate skin appendages (Sadier et al., 2014), including the density and patterning of bony armor derived from modified scales of several stickleback species (Colosimo et al., 2005; O'Brown et al., 2015), and the number of scales in Medaka (Kondo et al., 2001). The Eda pathway interacts with other important signaling pathways, including Hh, Wnt, FGF, and BMP, throughout skin appendage development of diverse vertebrates (Mikkola, 2008; Häärä et al., 2011, 2012). Therefore, a shift in Eda signaling may likely underlie the morphological evolution of the dermal skeleton in teleost groups, including the pufferfishes.

Conclusion

Members of the highly derived superorder Acanthopterygii possess astonishingly diverse scale morphologies. This diversity has arisen through acquisition of various ornamentations to the posterior region of the cycloid scale, such as tubercles, ridges, serrations, cteni, and spines (Sire, 1986). Tetraodontiformes constitute an exceptional example of scale evolution, particularly with respect to the spines observed in Tetraodontidae and Diodontidae. We suggest these spines are formed through the loss of the cycloid scale compartment present in the tetraodontiform ancestor, resulting in a reduced single spine, driven through modification of gene pathway signaling during scale development (such as Eda signaling; Figure 7). Tetraodontiform fishes have utilized this dermal system to develop a remarkable diversity of spine and scale morphologies. Together, our data suggest that Eda signaling may play a role in the evolutionary transition from spinoid scale to spine. Furthermore, shifts in expression of signaling pathways (such as Bmp) at various stages of appendage development have likely produced tremendous diversity in patterning and unit morphology in this group of derived teleost fishes. Future work on comparative expression patterns or transcriptome analyses may uncover a network of genes related to scale formation that can be directly compared with developing spines, potentially highlighting the genes lost or gained during the scale-to-spine transition.

Limitation of the Study

The *Takifugu* pufferfish breeding seasons are short, and this work could be performed only during 2 months of the summer season. We are now working on several pufferfish species to increase our knowledge of the development of these fishes.

METHODS

All methods can be found in the accompanying Transparent Methods supplemental file.

SUPPLEMENTAL INFORMATION

Supplemental Information can be found online at https://doi.org/10.1016/j.isci.2019.06.003.

ACKNOWLEDGMENTS

We thank members of the Fraser laboratory for comments on the manuscript and discussions and Serina Hayes for laboratory assistance. We are grateful to Hiroyuki Doi, Toshiaki Ishibashi, and Hisanori Kohtsuka for the donation of embryos. We also appreciate the open source CT scanning by members of the "Scan All Fishes" consortium, available at Morphosource.org, for the pufferfish scans (used for Figure 2), and we especially thank Adam Summers and Matt Kolmann (University of Washington, Friday Harbor Laboratories). This work was generously funded by the following research support: The Leverhulme Trust Research Project Grant RPG-211 (to G.J.F.), Natural Environment Research Council (NERC) Standard Grant

NE/K014595/1 (to G.J.F.), The Royal Society Research Grant RG120160 (to G.J.F.), The Great Britain Sasakawa Foundation (to G.J.F. and T.S.), the Daiwa Anglo-Japanese Foundation (to G.J.F.), and The Jikei University Graduate Research Fund (to M.O.). This work was also funded through "Adapting to the Challenges of a Changing Environment" (ACCE), an NERC-funded doctoral training partnership (to A.P.T.) ACCE DTP (NE/L002450/1).

AUTHOR CONTRIBUTIONS

T.S., D.K., A.P.T., and G.J.F. designed the research. T.S., D.K., A.P.T., R.B., and G.J.F. analyzed the data. T.S., D.K., A.P.T., R.L.C., R.B., M.O., and G.J.F. performed the research. T.S., R.L.C., A.P.T., R.B., and G.J.F. wrote the paper. All authors edited and agreed on the final version.

DECLARATION OF INTERESTS

The authors declare no competing interests.

Received: March 19, 2019
Revised: May 14, 2019
Accepted: June 1, 2019
Published: July 25, 2019

REFERENCES

Ahn, Y., Sanderson, B.W., Klein, O.D., and Krumlauf, R. (2010). Inhibition of Wnt signaling by Wise (Sostdc1) and negative feedback from Shh controls tooth number and patterning. Development *137*, 3221–3231.

Albertson, R.C., Kawasaki, K.C., Tetrault, E.R., and Powder, K.E. (2018). Genetic analyses in Lake Malawi cichlids identify new roles for Fgf signaling in scale shape variation. Commun. Biol. *1*, 55.

Aman, A.J., Fulbright, A.N., and Parichy, D.M. (2018). Wnt/β-catenin regulates an ancient signaling network during zebrafish scale development. Elife *7*, e37001.

Bauer, H., Meier, A., Hild, M., Stachel, S., Economides, A., Hazelett, D., Harland, R.M., and Hammerschmidt, M. (1998). Follistatin and Noggin are excluded from the zebrafish organizer. Dev. Biol. *204*, 488–507.

Biggs, L.C., and Mikkola, M.L. (2014). Early inductive events in ectodermal appendage morphogenesis. Semin. Cell Dev. Biol. *25–26*, 11–21.

Britz, R., Ali, A., Philip, S., Kumar, K., and Raghavan, R. (2012). First record from the wild of carinotetraodon imitator in Peninsular India (teleostei: Tetraodontiformes: Tetraodontidae). Ichthyol. Explor. Freshw. *23*, 105–109.

Colosimo, P.F., Hosemann, K.E., Balabhadra, S., Villarreal, G., Jr., Dickson, M., Grimwood, J., Schmultz, J., Mayers, R.M., Schluter, D., and Kingsley, D.M. (2005). Widespread parallel evolution in sticklebacks by repeated fixation of ectodysplasin alleles. Science *307*, 1928–1933.

Cooper, R.L., Martin, K.J., Rasch, L.J., and Fraser, G.J. (2017). Developing an ancient epithelial appendage: FGF signalling regulates early tail denticle formation in sharks. Evodevo *8*, 1–19.

Cooper, R.L., Thiery, A.P., Fletcher, A.G., Delbarre, D.J., Rach, L.J., and Fraser, G.J. (2018). An ancient Turing-like patterning mechanism regulates skin denticle development in sharks. Sci. Adv. *4*, eaau5484.

Cuny, G.D., Yu, P.B., Laha, J.K., Xing, X., Liu, J.F., Lai, C.S., Deng, D.Y., Sachidanandan, C., Bloch, K.D., and Peterson, R.T. (2008). Structure-activity relationship study of bone morphogenetic protein (BMP) signaling inhibitors. Bioorg. Med. Chem. Lett. *18*, 4388–4392.

Dal-Pra, S., Fürthauer, M., Van-Celst, J., Thisse, B., and Thisse, C. (2006). Noggin1 and follistatin-like2 function redundantly to chordin to antagonize BMP activity. Dev. Biol. *298*, 514–526.

Di-Poï, N., and Milinkovitch, M.C. (2016). The anatomical placode in reptile scale morphogenesis indicates shared ancestry among skin appendages in amniotes. Sci. Adv. *2*, 1–8.

Fessing, M.Y., Sharova, T.Y., Sharov, A.A., Atoyan, R., and Botchkarev, V.A. (2006). Involvement of the Edar signaling in the control of hair follicle involution (catagen). Am. J. Pathol. *169*, 2075–2084.

Fraser, G.J., Britz, R., Hall, A., Johanson, Z., and Smith, M.M. (2012). Replacing the first-generation dentition in pufferfish with a unique beak. Proc. Natl. Acad. Sci. U S A *109*, 8179–8184.

Gauldie, R.W. (1992). 'Plywood' structure and mineralization in the scales of the ocean sunfishes, *Mola mola* and *M. ramsayi*. Tissue Cell *24*, 263–266.

Geling, A., Steiner, H., Willem, M., Bally-Cuif, L., and Haass, C. (2002). A γ-secretase inhibitor blocks Notch signaling in vivo and causes a severe neurogenic phenotype in zebrafish. EMBO Rep. *3*, 688–694.

Grigoryan, T., Wend, P., Klaus, A., and Birchmeier, W. (2008). Deciphering the function of canonical Wnt signals in development and disease: conditional loss-and gain-of-function mutations of beta-catenin in mice. Genes Dev. *22*, 2308.

Häärä, O., Fujimori, S., Schmidt-Ullrich, R., Hartmann, C., Thesleff, I., and Mikkola, M.L. (2011). Ectodysplasin and Wnt pathways are required for salivary gland branching morphogenesis. Development *138*, 2681–2691.

Häärä, O., Harjunmaa, E., Lindfors, P.H., Huh, S.H., Flinjaux, I., Åberg, T., Jernvall, J., Ornitz, D.M., Mokkola, M.L., and Thesleff, I. (2012). Ectodysplasin regulates activator-inhibitor balance in murine tooth development through Fgf20 signaling. Development *139*, 3189–3199.

Harris, M.P., Rohner, N., Schwarz, H., Parathoner, S., Konstantinidis, P., and Nüsslein-Volhard, C. (2008). Zebrafish eda and edar mutants reveal conserved and ancestral roles of ectodysplasin signaling in vertebrates. PLoS Genet. *4*, e1000206.

Hovanes, K., Li, T.W., Munguia, J.E., Truong, T., Milovanovic, T., Lawrence Marsh, J., Holcombe, R.F., and Waterman, M.L. (2001). β-Catenin-sensitive isoforms of lymphoid enhancer factor-1 are selectively expressed in colon cancer. Nat. Genet. *28*, 53–57.

Incardona, J.P., Gaffield, W., Kapur, R.P., and Roelink, H. (1998). The teratogenic Veratrum alkaloid cyclopamine inhibits sonic hedgehog signal transduction. Development *125*, 3553–3562.

Iwasaki, M., Kuroda, J., Kawakami, K., and Wada, H. (2018). Epidermal regulation of bone morphogenesis through the development and regeneration of osteoblasts in the zebrafish scale. Dev. Biol. *437*, 105–119.

Jaillon, O., Aury, J.M., Brunet, F., Petit, J.L., Stange-Thomann, N., Mauceli, E., Bouneau, L., Fischer, C., Ozouf-Costaz, C., Bernot, A., et al. (2004). Genome duplication in the teleost fish Tetraodon nigroviridis reveals the early vertebrate proto-karyotype. Nature *431*, 946–957.

Jiang, T.X., Jung, H.S., Widelitz, R.B., and Chuong, C.M. (1999). Self-organization of periodic patterns by dissociated feather

mesenchymal cells and the regulation of size, number and spacing of primordia. Development *126*, 4997–5009.

Jung, H.S., Francis-West, P.H., Widelitz, R.B., Jiang, T.X., Ting-Berreth, S., Tickle, C., Wolpert, L., and Chuong, C.M. (1998). Local inhibitory action of BMPs and their relationships with activators in feather formation: implications for periodic patterning. Dev. Biol. *196*, 11–23.

Katayama, E., and Matsuura, K. (2016). Fine structures of scales of ocean sunfishes (Actinopterygii, Tetraodontiformes, Molidae): another morphological character supporting phylogenetic relationships of the Molid Genera. Bull. Natl. Mus. Nat. Sci. Ser. A *42*, 95–98.

Kondo, S., Kuwahara, Y., Kondo, M., Naruse, K., Mitani, H., Wakamatsu, Y., Ozato, K., Asakawa, S., Shimizu, N., and Shima, A. (2001). The medaka rs-3 locus required for scale development encodes ectodysplasin-A receptor. Curr. Biol. *11*, 1202–1206.

Lai, E.C. (2004). Notch signaling: control of cell communication and cell fate. Development *131*, 965–973.

Le Guellec, D., Morvan-Dubois, G., and Sire, J.Y. (2004). Skin development in bony fish with particular emphasis on collagen deposition in the dermis of the zebrafish (*Danio rerio*). Int. J. Dev. Biol. *48*, 217–231.

Matsuura, K. (2014). Taxonomy and systematics of tetraodontiform fishes: a review focusing primarily on progress in the period from 1980 to 2014. Ichthyol. Res. *62*, 72–113.

Mikkola, M.L. (2008). TNF superfamily in skin appendage development. Cytokine Growth Factor Rev. *19*, 219–230.

Mohammadi, M., McMahon, G., Sun, L., Tang, C., Hirth, P., Yeh, B.K., Hubbard, S.R., and Schiessinger, J. (1997). Structures of the tyrosine kinase domain of fibroblast growth factor receptor in complex with inhibitors. Science *276*, 955–960.

Mongera, A., and Nüsslein-Volhard, C. (2013). Scales of fish arise from mesoderm. Curr. Biol. *23*, R338–R339.

Mou, C., Jackson, B., Schneider, P., Overbeek, P.A., and Headon, D.J. (2006). Generation of the primary hair follicle pattern. Proc. Natl. Acad. Sci. U S A *103*, 9075–9080.

Musser, J.M., Wagner, G.P., and Prum, R.O. (2015). Nuclear β-catenin localization supports homology of feathers, avian scutate scales, and alligator scales in early development. Evol. Dev. *17*, 185–194.

Neubüser, A., Peters, H., Balling, R., and Martin, G.R. (1997). Antagonistic interactions between FGF and BMP signaling pathways: a mechanism for positioning the sites of tooth formation. Cell *90*, 247–255.

O'Brown, N.M., Summers, B.R., Jones, F.C., Brady, S.D., and Kingsley, D.M. (2015). A recurrent regulatory change underlying altered expression and Wnt response of the stickleback armor plates gene EDA. Elife *4*, 1–17.

Pan, Y., Lin, M.H., Tian, X., Cheng, H.T., Gridley, T., Shen, T., and Kopan, R. (2004). Gamma-secretase functions through Notch signaling to maintain skin appendages but is not required for their patterning or initial morphogenesis. Dev. Cell *7*, 731–743.

Pispa, J., and Thesleff, I. (2003). Mechanisms of ectodermal organogenesis. Dev. Biol. *262*, 195–205.

Plikus, M.V., Mayer, J., de la Cruz, D., Baker, E.R., Maini, P.K., Maxson, R., and Chuong, C.M. (2008). Cyclic dermal BMP signalling regulates stem cell activation during hair regeneration. Nature *451*, 340–344.

Roberts, C.D. (1993). Comparative morphology of spined scales and their phylogenetic significance in the Teleostei. Bull. Mar. Sci. *52*, 60–113.

Sadier, A., Viriot, L., Pantalacci, S., and Laudet, V. (2014). The ectodysplasin pathway: from diseases to adaptations. Trends Genet. *30*, 24–31.

Santini, F., and Tyler, J.C. (2003). A phylogeny of the families of fossil and extant tetraodontiform fishes (Acanthomorpha, Tetraodontiformes), upper cretaceous to recent. Zool. J. Linn. Soc. *139*, 565–617.

Shi, Y., and Massagué, J. (2003). Mechanisms of TGF-beta signaling from cell membrane to the nucleus. Cell *113*, 685–700.

Shimada, A., Kawanishi, T., Kaneko, T., Yoshihara, H., Yano, T., Inohaya, K., Knoshita, M., Kamei, Y., Tamura, K., and Takeda, H. (2013). Trunk exoskeleton in teleosts is mesodermal in origin. Nat. Commun. *4*, 1638–1639.

Sire, J.Y., and Akimenko, M.A. (2004). Scale development in fish: a review, with description of sonic hedgehog (shh) expression in the zebrafish (*Danio rerio*). Int. J. Dev. Biol. *48*, 233–247.

Sire, J.Y. (1986). Ontogenic development of surface ornamentation in the scales of *Hemichromis bimaculatus* (Cichlidae). J. Fish Biol. *28*, 713–724.

Thiery, A.P., Shono, T., Kurokawa, D., Britz, R., Johanson, Z., and Fraser, G.J. (2017). Spatially restricted dental regeneration drives pufferfish beak development. Proc. Natl. Acad. Sci. U S A *114*, E4425–E4434.

Thompson, T.B., Lerch, T.F., Cook, R.W., Woodruff, T.K., and Jardetzky, T.S. (2005). The structure of the follistatin: activin complex reveals antagonism of both type I and type II receptor binding. Dev. Cell *9*, 535–543.

Varjosalo, M., and Taipale, J. (2008). Hedgehog: functions and mechanisms. Genes Dev. *22*, 2454–2472.

Venkatesh, B., Gilligan, P., and Brenner, S. (2000). Fugu: a compact vertebrate reference genome. FEBS Lett. *476*, 3–7.

Vogel, A., Rodriguez, C., Warnken, W., Izpisúa Belmonte, J.C., and Izpisua Belmonte, J.C. (1995). Dorsal cell fate specified by chick Lmx1 during vertebrate limb development. Nature *378*, 716–720.

Yanagita, M. (2004). USAG-1: a bone morphogenetic protein antagonist abundantly expressed in the kidney. Biochem. Biophys. Res. Commun. *316*, 490–500.

ISCI, Volume ■ ■

Supplemental Information

Evolution and Developmental Diversity of Skin Spines in Pufferfishes

Takanori Shono, Alexandre P. Thiery, Rory L. Cooper, Daisuke Kurokawa, Ralf Britz, Masataka Okabe, and Gareth J. Fraser

Supplementary Materials

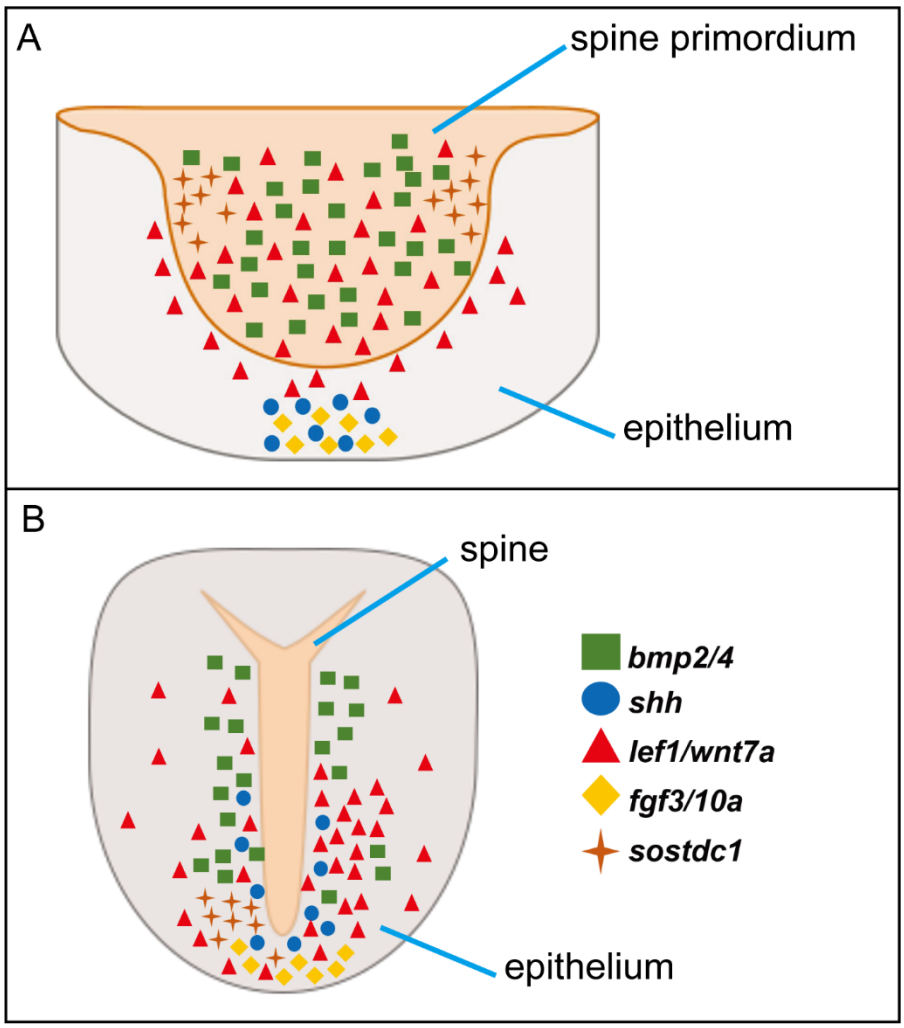

Figure S1 (related to Figure 4). Schematic diagram representing gene expression during morphogenesis of spines. Summary of gene expression patterns by whole mount and section *in situ* hybridization observed in *Takifugu* embryos at 12 dpf (A) where spine primordia form (seen in Figure 4) and 15 dpf (B) where spines develop during morphogenesis.

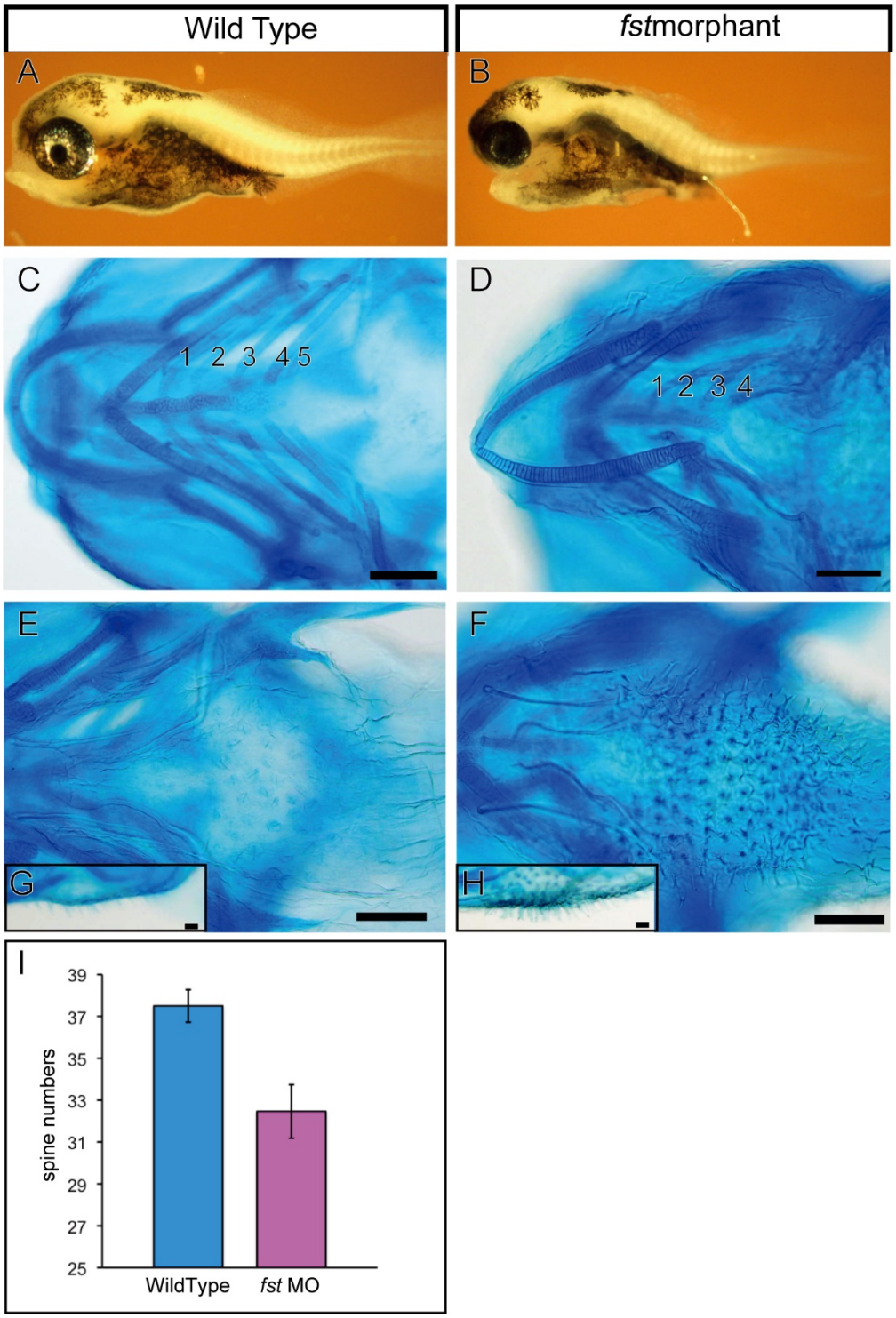

Figure S2. Hypertrophy of spine formation in *Takifugu* embryos after injection of *fst* morpholino (related to Figure 5 and 6). Wild type embryo (A, C, E and G) and a morphant with *fst* morpholino (*fst* MO) (B, D, F and H). (A and

B) Lateral view of embryos. (C-H) Embryos stained with Alcian Blue. (C) Dorsal view of craniofacial skeleton in wild type embryos showing the normal set of five branchial arches, (100%, n = 14). (D) Severe phenotype of a morphant showing an abnormal arrangement of Meckel's cartilage and only four branchial arches (18.2 %, n = 11). (E and F) Ventral view of embryos in the region of spine development. (G and H) Close up of spines in lateral view of embryos. (I) Quantitative comparison of the spine number per 2 mm^2 between embryos injected with control and *fst* MO. Spine number in *fst* MO is lower than that in wild type. Data are represented as mean ± SEM. Abbreviations: BB, basibranchial; 1-5, ceratobranchials 1-5; CH, ceratohyal; M, Meckel's cartilage. Scale bars, 100 μm (C-F), 50 μm (G and H).

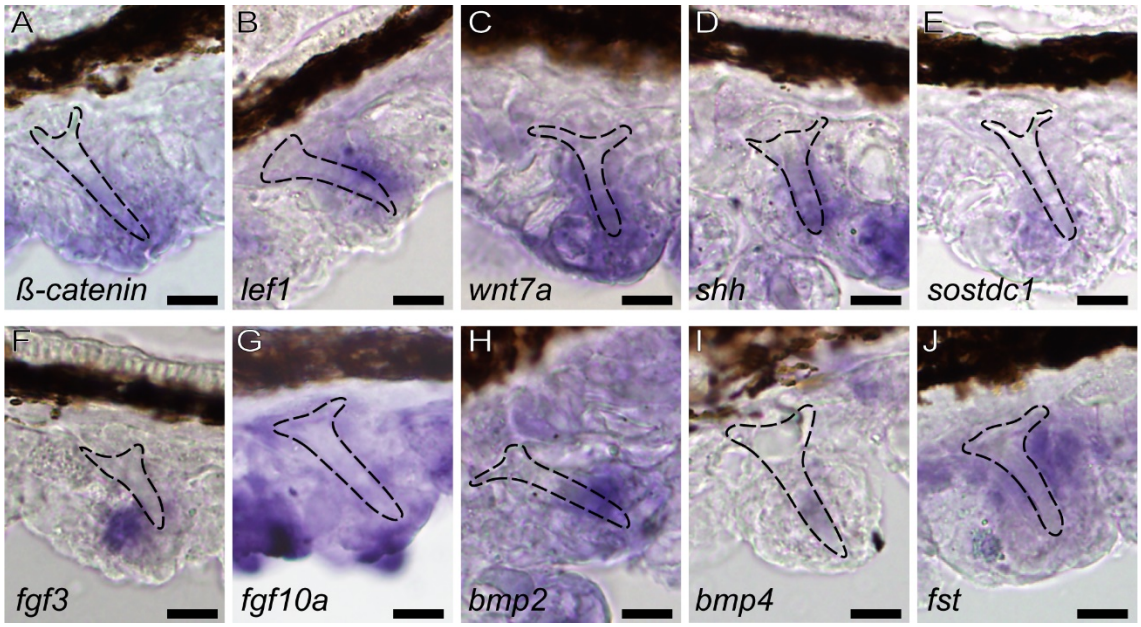

Figure S3 (related to Figure 4). Gene expression patterns during differentiation and development of spines. Transversal sections of hybridized spines in *Takifugu niphobles* embryos at 15 dpf illustrating the expression

patterns of *β-catenin* (A), *lef1* (B), *wnt7a* (C), *shh* (D), *sostdc1* (E)*, fgf3* (F), *fgf10a* (G), *bmp2* (H), *bmp4* (I) and *fst* (J). Black dotted lines indicate the individual spine each. (A-C) *β-catenin* and *wnt7a* are expressed in the epithelium uniformly surrounding spines, on the other hand, *lef1* is expressed in the posterior epithelia within the spine. (D) The expression of *shh* is more restricted within the epithelium compared to Wnt-related gene. (E) *sostdc1* is expressed in the epithelium anterior to the spine during morphogenesis. (F and G) *fgf3* and *fgf10a,* are extensively expressed in the epithelium adjacent distal tip of the spines. (H-J) *bmp2 and bmp4* are also extensively expressed the epithelium adjacent distal tip of spines, and *fst* is expressed within the epithelium around spines but not at the distal tip region. Scale bar, 25 μm.

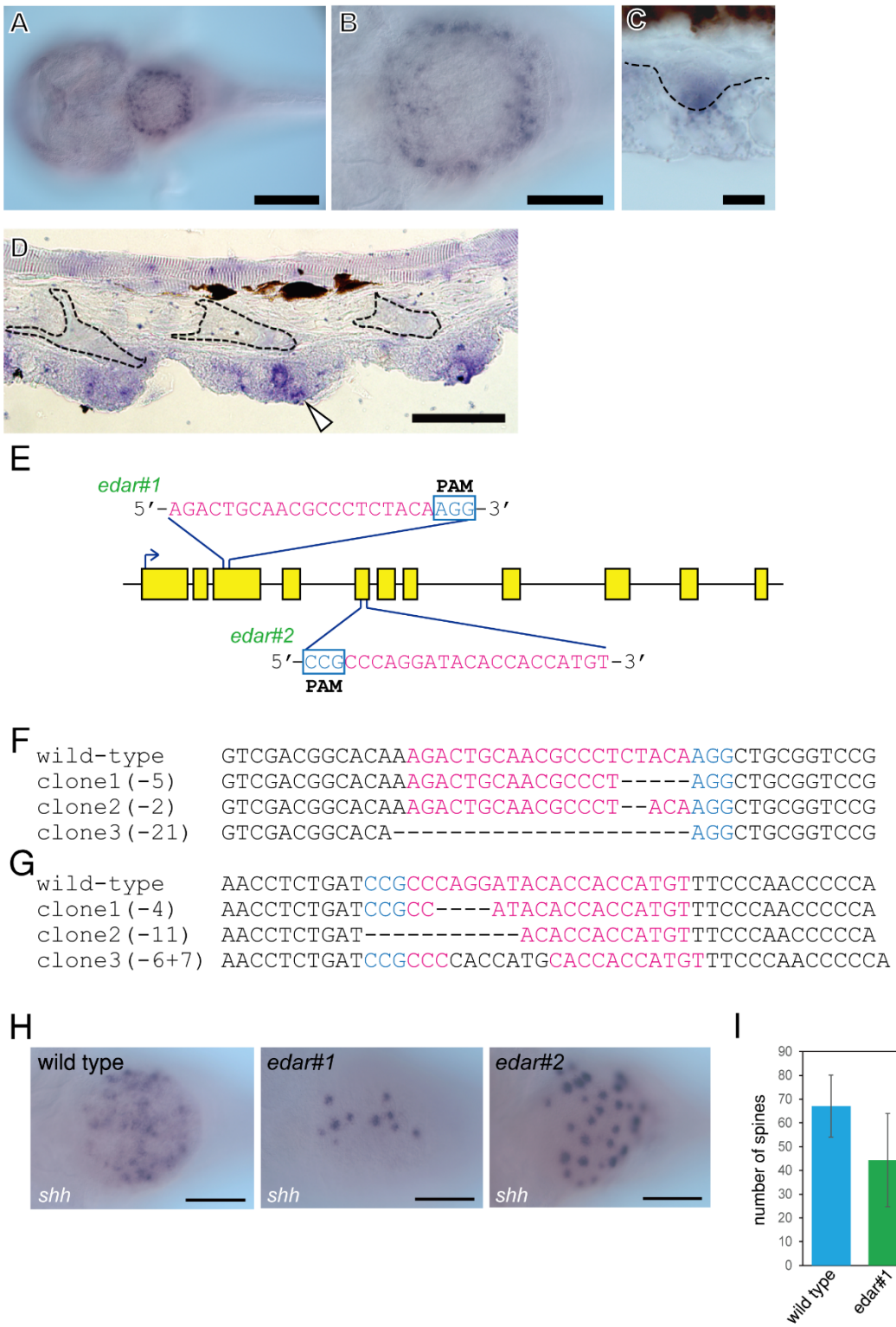

Figure S4 (related to Figure 4 and 6). Reduction in spine number of the G0 embryos of *Takifugu* by CRISPR/Cas9 targeted *edar*. (A-D) Gene expressions of *edar* during spine development in wild type embryos. (A and B) The ventral

view of an embryo with WISH showing for whole (A) and close up of spine regions (B). (C) Transverse section with SISH for spine primordia at 12 dpf. Black dotted lines indicate border between spine primordia and epithelium. (D) Transverse section with SISH for growth stage of spines in larvae at 50 dpf. Black dotted lines indicate the mineralized spines and white arrowhead indicates *edar* expressing cells at the tip of epithelium. (E) Schematic of two gRNA-Cas9 targeting the exons of *edar*, *edar#1* for exon3 and *edar#2* for exon5. The target sequence and PAM sequence are highlighted in red and blue respectively. (F and G) Insertion and deletion in the CRISPR-Cas9 targeted *edar* revealed by sequencing for *edar#1* (C) and *edar#2* (D). (H) Gene expressions of *shh* in wild-type and *edar* mutated embryos, *edar#1* and edar#2 at 12 dpf. Close up ventral view of embryos showing spine primordium express *shh*. (I) Quantitative comparison of the spine number between embryos of wild-type and *edar* mutated embryos (*edar#1* and *edar#2*). Spine number in *edar#1* is lower than that in wild type. Data are represented as mean ± SEM. Scale bars, 100 μm (A and B), 10 μm (C), 50μm (D)

Family	Larval stage		Adult stage	
	cycloid	spinoid	cycloid	spinoid
Triacanthodidae	+	+	+	+
Triacanthidae	+	+	+	+
Balistidae	+	+	+	+
Monacanthidae	+	+	+	+
Aracanidae	N/A	N/A	+	-
Ostraciidae	+	-	+	-
Triodontidae	+	+	+	+
Tetraodontidae	-	+	-	+
Diodontidae	-	+	-	+
Molidae	-	+	+	-

Table S1 (related to Figure 1). List of scale structures amongst Tetraodontiformes. The scale typically consists of two regions, an anterior "cycloid" plate and posterior spinous structures. Adult scale morphology as observed in a published data (Matsuura, 2014).

Chemical	Concentration	Blocking pathway	sample number	Spine numbers (Average±SEM)
DMSO	1%	n/a	5	142.4±6.56
Cyclopamine	50 μM	Hh	6	75.17±12.28
DAPT	25 μM	Notch	9	89.67±5.07
LDN	5 μM	Bmp	9	122.78±3.12
SU5402	50 μM	Fgf	10	120.5±4.06
IWR-1	1 μM	Wnt	1	27±0

Table S2 (related to Figure 6). List of chemical perturbation experiments to inhibit signaling pathways during the development of spines. The phenotype in chemically treated embryos are reported by calculating average number of spines. Abbreviation; SEM, Standard error of the mean.

Familly	Species	Collections	Standard Length (mm)	Stage
Triacanthodidae	*Hollardia* sp.	BMMH	5.0	larvae/juvenile
	Paratriacanthodes herrei	BMNH	42.5	adult
Triacanthidae	*Tripodichthys oxycephalus*	BMNH	4.3	larvae/juvenile
	Pseudotriacanthus strigilifer	BMNH	88.0	adult
Balistidae	*Balistes vetula*	MCZ	10.0	larvae/juvenile
	B. capriscus	BMNH	128.0	adult
Monacanthidae	*Stephanolepis* sp.	SEAMAP	5.0	larvae/juvenile
	S. hispidus	BMNH	94.5	adult
Ostraciidae	*Ostracion* sp.	BMNH	6.2	larvae/juvenile
	Ostracion trigonus	BMNH	330.0	adult
Triodontidae	*Triodon macropterus*	MNHN	20.0	larvae/juvenile
	T. macropterus	BMNH	315.0	adult
Tetraodontidae	*Takifugu niphobles*	BMNH	10.0	larvae/juvenile
	Takifugu niphobles	BMNH	102.3	adult
Diodontidae	*Diodon holocanthus*	BMNH	12.5	larvae/juvenile
	D. holacanthus	BMNH	101.0	adult
Molidae	*Ranzania laevis*	BMNH	1.7	larvae/juvenile
	R. laevis	BMNH	620.0	adult

Table S3. List of species used in this study for clearing and staining represented in Figure 1. Institution abbreviation used in Table: Natural History Museum London (BMNH), Museum of Comparative Zoology, Harvard (MCZ), Muséum national d'histoire naturelle, Paris (MNHN) and Southeast Area Monitoring and Assessment Program Ichthyoplankton Archiving Center, Fish and Wildlife Research Institute (SEAMAP).

Transparent Methods

Animals

Eggs of the pufferfish *Takifugu niphobles* and juveniles of the filefish *Stephanolepis cirrhifer* were collected on Arai beach, Kanagawa prefecture, Japan. *Takifugu* eggs were raised to desired embryonic stages in fresh seawater at 20°C. Collections of *Diodon holocanthus* juveniles fixed with 10% formalin in seawater were supplied by Shimonoseki Marine Science Museum. Our comparative cleared and double stained methods were performed on tetraodontiform material obtained from the collection at the Natural History Museum London, and includes the species; *Hollardia sp*. and *Paratriacanthodes herrei* (Triacanthodidae), *Tripodichthys oxycephalus* and *Pseudotriacanthus strigilifer* (Triacanthidae), *Balistes vetula* and *B. capriscus* (Balistidae), *Stephanolepis sp*. and *S. hispidus* (Monacanthidae), *Ostracion sp*. and *O. trigonus* (Ostraciidae), *Triodon macropterus* (Triodontidae), *Takifugu niphobles* (Tetraodontidae), *Diodon holocanthu* (Diodontidae) and *Ranzania laevis* (Molidae). Species used in this study are listed in Table S3.

Histology and clearing and double staining

Takifugu embryos for histology staining were fixed in 4% paraformaldehyde in PBS (Phosphate Buffered Saline) at 4°C overnight and dehydrated in a graded series of methanol. For paraffin embedding, dehydrated samples were incubated 20 minutes with isopropanol and two times for 30 minutes with Histo-Clear. Leica RM2145 microtome was used to section paraffin embedded samples at 14 µm.

Slides were stained with 50% haematoxylin for 10 minutes and Alcian Blue solution (0.01% Alcian Blue, 70% ethanol and acetic acid) for 30 minutes. Stained slides were washed with double distilled water and mounted with Fluoromount (SIGMA). Finally mounted slides were photographed by using a BX51 Olympus compound microscope equipped with an Olympus DP71 camera.

Takifugu embryos and juveniles for clearing and staining were breached with breaching solution (1% H_2O_2, 5% formamide, 0.5x SSC, 75 mM NaCl, and 7.5 mM sodium citrate, pH 7.0). For Alizarin Red staining juveniles were placed into 0.5% trypsin solution at room temperature for overnight. After protein digest, calcified tissues were stained using 0.01% Alizarin Red S in 0.5%KOH solution for 3 hours. Cartilages were stained with Alcian Blue solution for overnight, and spines were also observed in the cartilage stained preparations. Cleared and stained fishes were washed with 0.5%KOH then graded into 80% glycerin. Additional specimens illustrated in Figure 1 were prepared according to a published protocol (Taylor and Van Dyke, 1985).

Scanning electron microscopy

Takifugu embryos were fixed in 4% paraformaldehyde in PBS at 4°C overnight and dehydrated in a graded series of methanol. The embryos were critical-point dried using liquid CO_2, mounted on a sample holder, covered with gold, and viewed using a Philips XL-20 scanning electron microscope.

Microinjections

Antisense morpholinos (MOs) were injected into *Takifugu* eggs with a micro needle using an injector NARISHIGE IM 300 (NARISHIGE). 0.8 mM MOs against *fst* (*follistatin*) (5'–TTCAGCATCCCAAACATGATGGAGC-3') were injected into 1cell stage of *Takifugu* eggs.

Designing of gRNA targeting* edar *and preparation for gRNA-Cas9 solution

CRISPR direct (https://crispr.dbcls.jp/) were used to design gRNA targeting *edar* exons for *Takifugu.* Specifity check were selected Fugu genome (*Takifugu rubripes*), FUGU5/fr3 (Oct, 2011) to predict potential of off target sites. Two gRNA with highest on target activity and lowest predict off target score was selected for the experiments. The selected two gRNA sequences were: gRNA *edar*#1; 5'-AGACTGCAACGCCCTCTACA -3' and gRNA *edar#2*; 5'-ACATGGTGGTGTATCCTGGG -3'. Synthesized gRNA, tracrRNA and CAS9 protein were purchased from IDT (Integrated DNA Technologies, Inc. The mixture of solution for the microinjection were prepared by the protocol provided from IDT (http://sfvideo.blob.core.windows.net/sitefinity/docs/default-source/user-submitted-method/crispr-cas9-rnp-delivery-zebrafish-embryos-j-essnerc46b5a1532796e2eaa53ff00001c1b3c.pdf?sfvrsn=52123407_10). To test whether insertion/deletion of genomic locus were occurred, PCR were performed to amplify the clone of gRNA target sites from injected embryos at 10 dpf. The sequence of primers for PCR were following,

edar#1-F: 5'- GAAATCTGTCGACGGCACA -3'

edar#1-R: 5'- CAGGTAAACAGGGTCCACAC -3'

edar#2-F: 5'- GTCCACCAGTGTGCCAAAAG -3'

155 *edar#2*-R: 5'- GCTGTTGGGCTTGGCTTTA -3'

156 Post injected embryos with whole-mount or section *in situ* hybridization were
157 imaged by Zeiss Axiocam 512 color under a Zeiss Axio Imager D1 compound
158 microscope

159

160 ***Molecular cloning and probe synthesis***

161 Total RNA was extracted from whole bodies of *Takifugu* (7 dpf) in RNA later
162 (Sigma) were transferred to TRIzol (Invitrogen) and washed with RNeasy cleanup
163 kit (Qiagen). Single-stranded cDNA was synthesized from total RNA using a
164 RETROscript Reverse Transcription Kit (Ambion) according to the
165 manufacturer's instructions. The sequence of genes was identified from the
166 genome database available at the International Fugu Genome Consortium
167 (http://www.fugu-sg.org/project/info.html). *Takifugu* cDNA clone of *β-catenin*
168 (LC483846), *lef1* (LC483847), *wnt7a* (LC483848), *shh* (LC483849), *sostdc1*
169 (LC483850), *fgf3* (LC483851), *fgf10a* (LC483852), *bmp2* (LC483853), *bmp4*
170 (LC483854), *fst* (LC483855), *notch3* (LC483856) and *edar* (LC483857) were
171 isolated by PCR using following forward and reverse primes designed from
172 Takifugu rubripes genomic sequence: *β-catenin*, 5'-
173 CCCTGAGGAAGATGATGTGGACAA-3' and 5'-
174 ACAGTTCTGGACCAGTCTCTGGCTG-3'; *lef1*, 5'-
175 CAGTCCCAAATACCAGATTCATATC-3' and 5'-
176 TCTTCTTCTTTCCATAGTTGTCTCG-3'; *wnt7a*, 5'-
177 CTTTGTCTGGGAATTGTCTATTTG-3' and 5'-
178 AGGTGTTGCATTTAACGTAGCAG-3'; *shh*, 5'-

GAAGGCAAGATCACAAGAAACTC-3’ and 5’-ACGTTCCCACTTGATAGAGGAG-3’; *sostdc1*, 5’-TCTCTGGTCCTCCTCGTGTC-3’ and 5’- CGACTGGTTGTGGTGAGCCC-3’; *fgf3*, 5’- GTTGAATTTGTTGGATCCGGTTAG-3’ and 5’-TGACCTTCGTCTCTTAACTCTCTTG-3’; *fgf10a*, 5’-GTGTAGATGGACAGTGACACAAGG-3’ and 5’-TTCTTGTTGCGCCACTCCGCCGAG-3’; *bmp2*, 5’-TTAGAAGCTTTCACCATGAAGAGTC-3’ and 5’-TTCATCCAGGTAGAGTAAGGAGATG-3’; *bmp4*, 5’-AGAACAACCATGCTAGTCTGATA-3’ and 5’-GTGGCAGTAATAGGCTTGATAACC-3’; *fst*, 5’-CTCTTGTTCATGTGGCTTTGTC-3’ and 5’-AGTCTGAGTCCTCATCTTCATCATC-3’; *notch3*, 5’-TCTGACTACACTGGAAGCTATTGTG-3’ and 5’-TTGCAGTCAAAGTTGTCATAGAGAC-3’; *edar*, 5’-GTACTCCAAAGGGAAGTACGAAATC-3’ and 5’-AAGATCTTTCTCCTCCGACTCTG-3’.

The PCR clone in the pGEM-T-Easy Vector (Promega) was used as a template, and a digoxigenin (DIG)-labeled antisense RNA probe was synthesized by in vitro transcription with T7/SP6 RNA polymerase (Promega) and DIG RNA labeling mix (Roche).

Whole mount and section* in situ *hybridization

All *Takifugu* embryos for *in situ* hybridization were fixed in 4% paraformaldehyde

in 0.01 M PBS at 4°C overnight. Fixed samples were dehydrated with graded series of methanol. Whole mount *in situ* hybridization was performed according to a published protocol (Shono et al., 2011). Section *in situ* hybridization was carried out on paraffin sections, they were de-paraffinized, rehydrated and superheated with 10 mM citric acid in diethylpyrocarbonate (DEPC) treated double distilled H_2O (pH 6). Slides were incubated in hybridization buffer (50% formamide, 5x SSC (Saline Sodium Citrate), 500 mg/ml yeast tRNA, 50 mg/ml heparin, and 0.01% Tween-20, pH 6.0) containing DIG-labeled antisense RNA probe at 61°C overnight. The hybridized slides were washed 1hour with 2xSSCT (Saline Sodium Citrate and 0.01% Tween-20, pH7.0) and three times for 30 minutes with 0.2xSSCT at 51°C. After incubation for 1 hour with blocking solution (2% Blocking Reagent (Roche) in MABT) at room temperature, slides were immunoreacted overnight at 4°C with an anti-DIG Fab fragment conjugated to alkaline phosphate (Roche, 1:5000). After several washes for 6 hours with MABT (100 mM maleic acid, 150 mM NaCl, and 0.01% Tween 20, pH 7.5) and two washes with NTMT (100 mM NaCl, 50 mM $MgCl_2$, 100 mM Tris-HCl (pH 9.5), and 0.01% Tween-20), samples were treated with BM purple AP Substrate precipitating solution (Roche). When satisfactory coloration was achieved, slides were washed with double distilled water and mounted with Fluoroshield with DAPI (SIGMA).

Treatment with small-molecules

Stock solutions were prepared for each chemical treatment experiment using Dimethyl Sulfoxide (DMSO) as a solvent. All treatment of small molecules were

based on and adapted from a published data (Plikus et al., 2008). 8 dpf *Takifugu* embryos were split into small molecules in sea water for 3 days. Final concentration of small molecules (Cyclopamine, DAPT, LDN193189, SU5402 and Iwr-1 (MedChem Express)) are shown in Table S2. After the treatment, embryos for *in situ* hybridization were fixed and for clearing and staining were washed extensively with sea-water and were raised for 4 days prior to sacrifice and fixation. The number of ventral spines was counted under a BX51 Olympus compound microscope.

Supplemental References

Plikus, M. V., Mayer J, de la Cruz, D., Baker, E. R., Maini, P. K., Maxson, R. and Chuong. C, M. (2008) Cyclic dermal BMP signalling regulates stem cell activation during hair regeneration. Nature 451, 340–344.

Matsuura, K. (2014) Taxonomy and systematics of tetraodontiform fishes: a review focusing primarily on progress in the period from 1980 to 2014. Ichthyol. Res 62, 72–113.

Shono, T., Kurokawa, D., Miyake, T. and Okabe, M. (2011) Acquisition of glial cells missing 2 enhancers contributes to a diversity of ionocytes in zebrafish. PLoS One 6, 1–9.

251 Taylor, W. and Van Dyke, G. C. (1985) Revised procedures for staining and
252 clearing small fishes and other vertebrates for bone and cartilage study. Cybium
253 9, 107–119.